

Electromagnetic behavior of in-situ synthesized MXene-based $\text{Ti}_3\text{C}_2/\text{TiO}_2$ composites

Kh. Zamani, M. Tavoosi*, A. Ghasemi

Department of Materials Engineering, Malek-Ashtar University of Technology (MUT), Iran

Email: ma.tavoosi@gmail.com

Tel./Fax: +983134429844

Abstract

The present work, set out with the aim of studying the effect of in-situ precipitation of TiO_2 from $\text{Ti}_3\text{C}_2\text{T}_x$ MXene phase on the electromagnetic (EM) behavior of $\text{Ti}_3\text{C}_2/\text{TiO}_2$ composites. In this regard, $\text{Ti}_3\text{C}_2\text{T}_x$ MXene phase was synthesized using HF acidic etching of Ti_3AlC_2 MAX phase and the in-situ precipitation of TiO_2 phase within Ti_3C_2 sheets was followed by controlled annealing in temperature range of 500-800 °C for 2 h. The phase and structural characteristics of prepared composites were investigated using X-ray diffraction (XRD), scanning electron microscope (SEM) and differential thermal analysis. The electromagnetic behavior of samples was also analyzed using vector network analyzer (VNA). The results showed that by performing the controlled annealing process of $\text{Ti}_3\text{C}_2\text{T}_x$ MXene phase, it is possible to in-situ formation of TiO_2 phase and form the $\text{Ti}_3\text{C}_2/\text{TiO}_2$ composites. The electromagnetic behavior of $\text{Ti}_3\text{C}_2/\text{TiO}_2$ composites is in direct relation with the percentage of TiO_2 phase deposited within Ti_3C_2 sheets during annealing process. The reflection loss (RL) changed from -7.98 to -21.28 dB (within frequency range of 1-18 GHz) with increasing in annealing temperature from 500 to 800 °C as well as increasing the size and percentage of formed TiO_2 particles.

Keywords: MAX; MXene; In-situ; composite; Electromagnetic.

1. Introduction

High temperature electromagnetic wave absorbing materials thanks to their wide applications- have attracted the attention of scientific research societies. These materials have secured their place in communication means/devices, aerospace industries and electronic equipment [1]. Besides exhibiting high performance in waves absorbing, they should have very slight thickness, light weight and a wide frequency range [2]. Traditional wave absorbing materials including ferrites, metallic magnetic powders, conducting polymers, etc. faced limitations and did not meet these requirements. Hence, the development of new materials with the unique properties such as MAX and MXenes was accelerated [3].

MXenes are known by the general formula of $M_{n+1}AX_n$ ($n=1,2$ or 3) generated by selective etching of MAX phase ceramics. In this formula, M is an intermediate metal, A is an element from group A (often an element from groups 3, 4 or 5 of periodic table), X is nitrogen or carbon and T_x representing superficial functional groups like -F, -OH, and -O [4, 5]. This group of materials, owing to their layered structure and a large number of native defects and chemically active surfaces, are most apt candidates for EM interference shielding and absorption applications [6].

Based on literatures, the shielding performance of MXenes can be improved by adding magnetic and dielectric reinforcing phases. However, dielectric reinforcement materials are more desirable for high temperature applications, as the magnetic properties of the material are lost at high temperatures [7-9]. In this regard, a large number of research works have been devoted to the investigation of MXene based composites containing dielectric materials [10]. Among the dielectric absorbent materials, TiO_2 is a suitable candidate for high temperature EM applications due to its stable dielectric property and low density. Also TiO_2 brings about an increase in $Ti_3C_2T_x$ MXene dielectric layers optimizing the impedance matching [11].

Moreover, TiO_2 can be deposited in-situ inside the MXene layers during a controlled annealing [12-14].

In this regard, Fan et al. [15] reported that the precipitation of TiO_2 nanoparticles from $\text{Ti}_3\text{C}_2\text{T}_x$ during annealing process has significant effects on EM absorption behaviors of prepared composites. In this research, the RL_{min} of prepared $\text{Ti}_3\text{C}_2\text{T}_x/\text{TiO}_2$ composite was reached to about 40.7 in matching frequency of 19.2 GHz (thickness 1.5 mm). In other work, Sun et al. [16] successfully grew TiO_2 particulate inside $\text{Ti}_3\text{C}_2\text{T}_x$ MXene layers using hydrothermal method and achieved the reflection loss of about 58.30 dB (1.75 mm thickness) in optimized composite. Reports presented by Gao et al. [18] and Yan et al. [17] also show the positive effects of the presence of TiO_2 on EM behavior of MXene based composites within band X boundary.

Despite the numerous studies about the preparation and different characteristics of MXene based composites, no coherent report has yet been presented on the exact effect of TiO_2 on the EM behaviors of these composites. So, this research focused on the in-situ preparation of TiO_2 phase within Ti_3C_2 sheets during controlled annealing process of $\text{Ti}_3\text{C}_2\text{T}_x$ MXene phase. The most important goal of this work was to investigate the electromagnetic wave absorption behavior in the frequency range of L (1 to 2 GHz), S (2 to 4 GHz), C (4 to 8 GHz), X (8 to 12 GHz) and Ku (12 to 18 GHz) bands in the formed composites.

2. Experimental procedure

In this research, Ti_3AlC_2 MAX powder with a purity of above 99% and a mean particle size of less than 10 μm (REDOX company) were used as raw materials for the formation of MXene phase. The $\text{Ti}_3\text{C}_2\text{T}_x$ MXene phase was prepared using selective etching of Al from the Ti_3AlC_2 MAX powder in the Hydrofluoric acid (HF) (≥ 40 wt%, analysis) [11]. In a typical synthesis process, 2 g of the MAX powders were slowly added to 50 mL of HF solution. The etching

process was continued for 24 h [19], while stirring proceeded with the help of a magnetic bar. Afterwards, the mixture was washed several times with deionized water whereupon centrifugation performed at 3500 rpm for 5 min per cycle. After the last centrifuge, the pH of the supernatant was around 7.0. Subsequently, the product was washed with alcohol and dried in a vacuum oven at 60 °C for 24 h [19]. The Ti₃C₂/TiO₂ composites were prepared during controlled annealing process of prepared Ti₃C₂T_x MXene phase at temperature range of 500-800 °C for 2 h (under argon protective atmosphere).

Phase examinations of the obtained samples were done via X-ray diffraction (XRD) analysis by utilizing XRD device (PW3710, Phillips Co.) under voltage 40 kV and current 0.05 Ampere. Morphological characteristics of the powder samples were inspected through scanning electron microscopy (SEM) (VEGA-TESCAN-XMU, Czech Republic). The differential scanning calorimetry (DSC) analysis of the samples was also conducted using STA 409 PC/PG device (NETZSCH Co.), under argon gas protection with the heating rate of 20 °C/min. A PNA-5222A vector network analyzer (VNA) system was utilized for analyzing the electromagnetic waves absorption of the studied samples.

3. Results and discussion

The X-ray diffraction patterns of Ti₃AlC₂ MAX phase before and after etching process at HF solution for 24 h are shown in Fig. 1. A glance at the peaks formed in Fig. 1 (a) at angles of 34.1, 36.8, 38.9, 41.9, and 74.2° based on the reference code (JCPDS:52-0875) indicates the formation of a high-purity Ti₃AlC₂ MAX phase and there is no evidence of impurities in this sample. Fig. 1 (b) shows the XRD pattern of Ti₃AlC₂ MAX phase after selective etching of Al in HF solution for 24 h. As can be clearly seen, the diffraction peaks corresponding to the Ti₃AlC₂ phase completely disappear and the XRD pattern is formed at angles of 18.5, 35.9, 41.7 and 60.7° corresponding to the characteristic peaks of the Ti₃C₂T_x MXene phase [11, 20]. The latter result is confirmed by the SEM micrographs illustrated in Fig. 2, where the

accordion-like multi-layered nano-flake $Ti_3C_2T_x$ MXene is clearly visible. The result obtained from SEM image is consistent with those presented by Tong et al. [21].

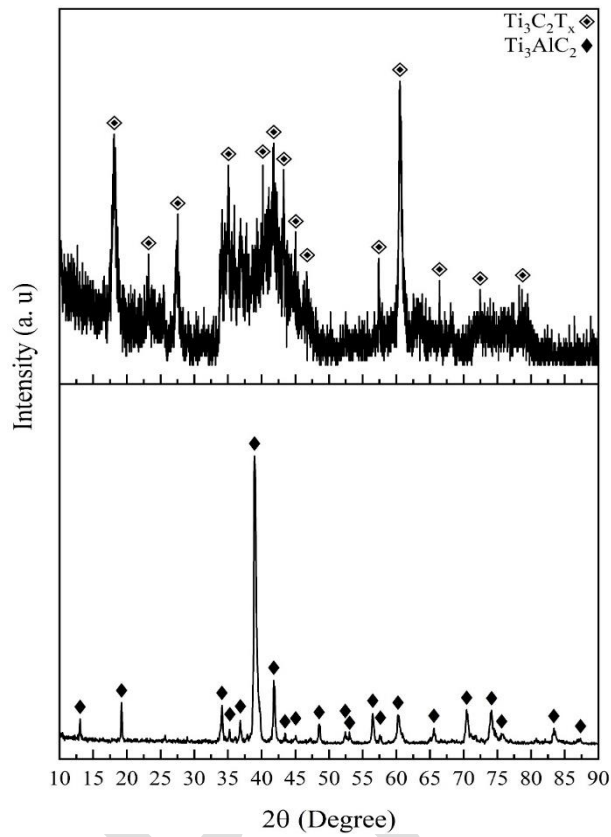
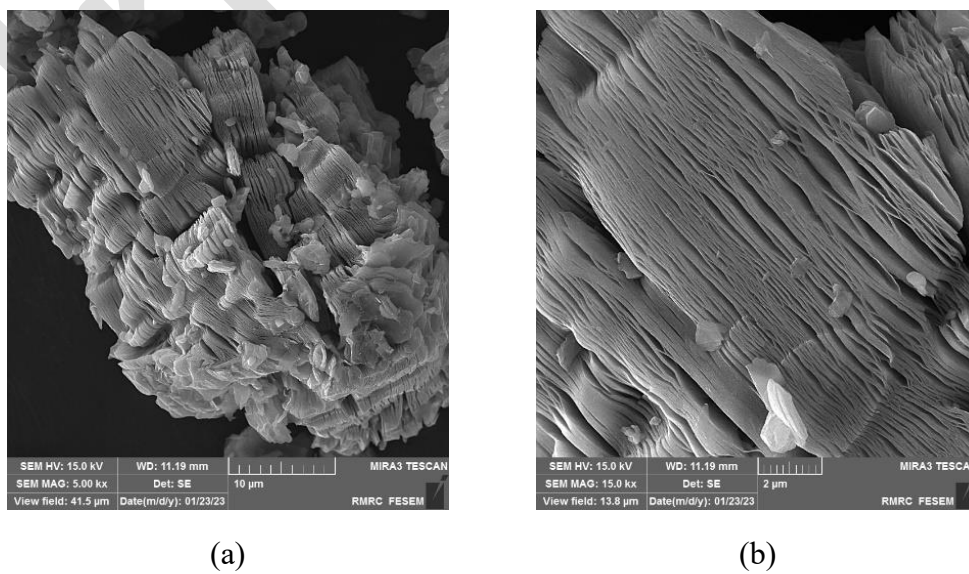


Fig.1. X-ray diffraction patterns of Ti_3AlC_2 MAX phase a) before and b) after etching process in HF solution for 24 h.

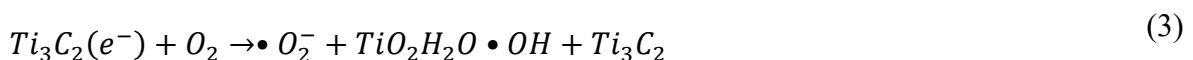
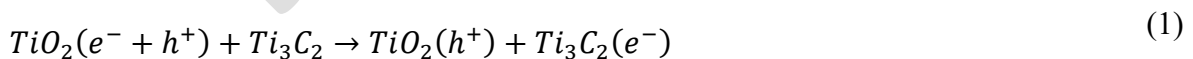


(a)

(b)

Fig.2. the SEM micrographs of Ti_3AlC_2 MAX phase after etching process in HF solution for 24 h (at two different magnifications).

In order to study the thermal behavior of prepared $Ti_3C_2T_x$ MXene phase, the sample was examined using DSC technique under continuous heating. The DSC heating trace of this sample, in Fig. 3, reveals only one wide endothermic peak at temperature range of 500-800 °C. To analyze the phase transformation responsible for the endothermic peak, the $Ti_3C_2T_x$ MXene phase was annealed within 500, 600, 700 and 800 °C for 2 h and the samples were examined using XRD technique. The XRD patterns of annealed samples are presented in Fig. 4. As seen, during annealing process, the diffraction peaks intensity corresponding to MXene phase gradually decrease and several new peaks related to TiO_2 phase with anatase at 25.1, 37.5, 48.12, 54.7, and 69.56 ° angles (JCPDS:21-1272) and TiO_2 phase with rutile at 27.4, 36.06, 41.22, 54.32, and 56.7° angles (JCPDS:21-1276) structures appear in XRD patterns. This finding is in agreement with those reported by Lei et al. [22]. Therefore, the endothermic peak in Fig. 3 should be attributed to the precipitation of TiO_2 from the $Ti_3C_2T_x$ MXene phase. In fact, the presence of -OH and -O groups on the surface of $Ti_3C_2T_x$ causes thermodynamic instability of MXene and leads to the in-situ formation of TiO_2 deposits during annealing process [23, 24]. The following equations (1-5) can be proposed to explain the formation mechanism of Ti_3C_2/TiO_2 composite:



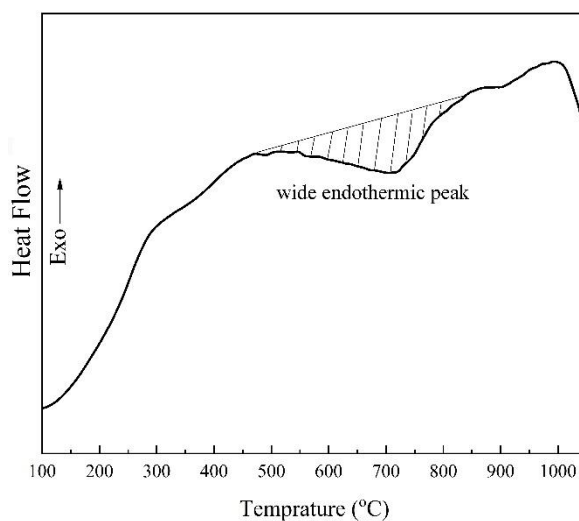
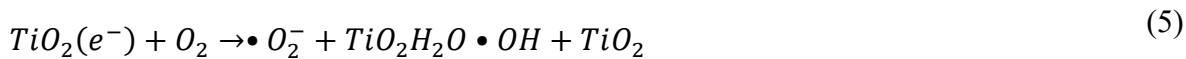


Fig.3. The DSC heating trace of $Ti_3C_2T_x$ MXene phase.

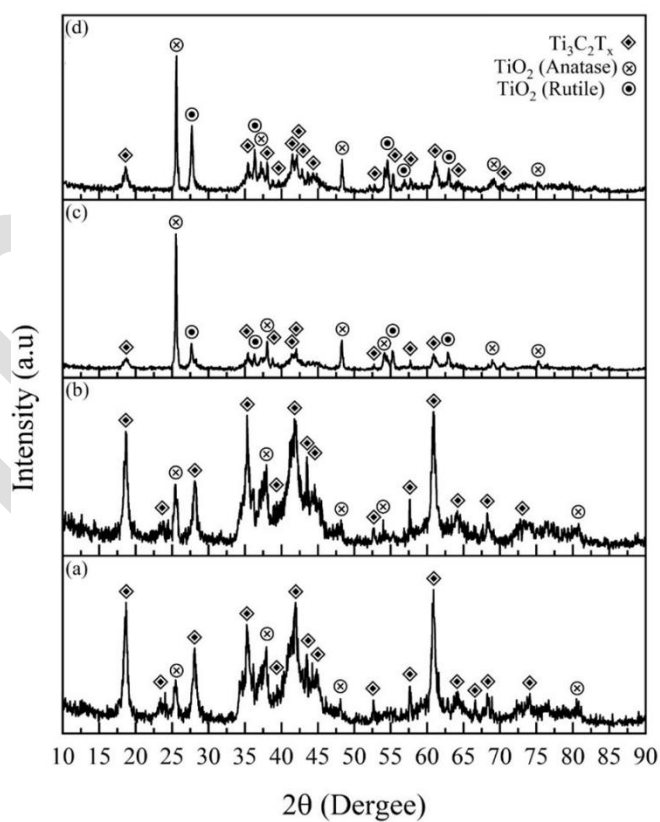
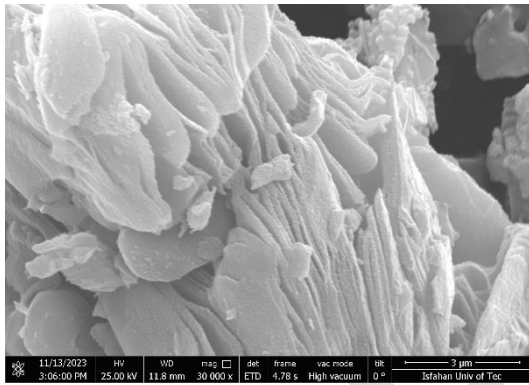
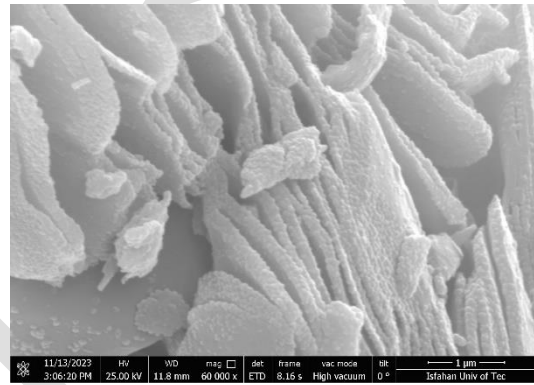


Fig. 4. X-ray diffraction patterns of $Ti_3C_2T_x$ MXene phase after annealing process at, a) 500, b) 600, c) 700 and d) 800 °C for 2 h.

As mentioned, the diffraction patterns presented in Fig. 4 well confirm the in-situ formation of $\text{Ti}_3\text{C}_2/\text{TiO}_2$ composites. This result is in agreement with the presented SEM micrographs of annealed samples at 500, 600, 700 and 800 °C in Fig. 5. Based on this figure, the nano-sized TiO_2 particles with unique distribution are formed on initial layers of MXene sheets. The morphology of formed TiO_2 nano-particles is closed to spherical and their size increases to about 180 nm with increasing annealing temperature.



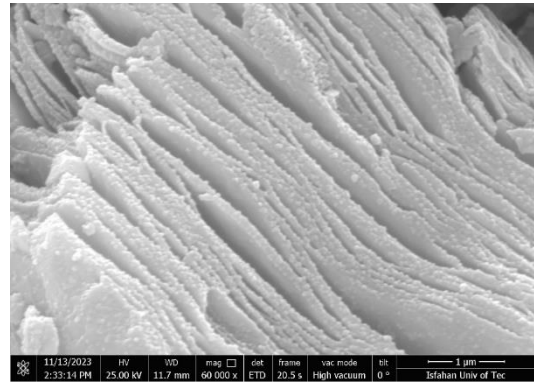
(a)



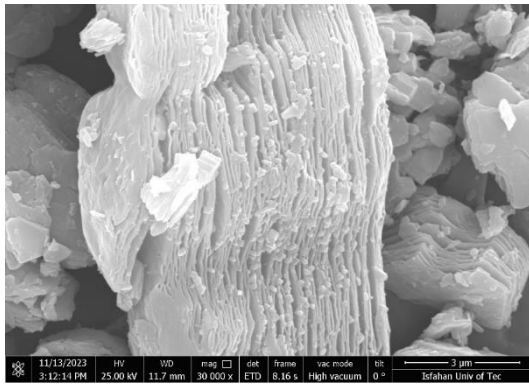
(b)



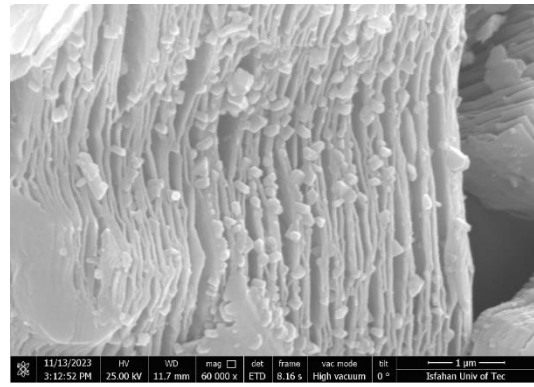
(c)



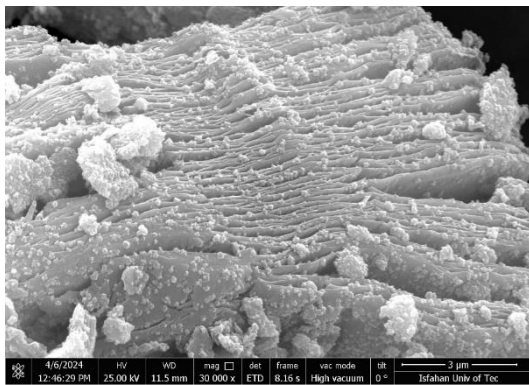
(d)



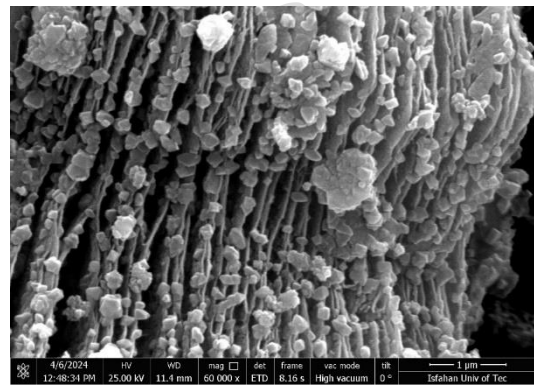
(e)



(f)



(g)



(h)

Fig. 5. The SEM micrographs of $Ti_3C_2T_x$ MXene phase after annealing process at, a & b) 500, c & d) 600, e & f) 700 and g & h) 800 °C for 2 h.

Real parts of electrical permittivity (ϵ') and magnetic permeability (μ') indicate electrical and magnetic energy storage potential. Whereas imaginary parts show rate of electrical and magnetic energy loss [25]. The real (μ') and imaginary parts (μ'') of permittivity in prepared composites in this study are evaluated about 1 and 0, respectively as a result of the absence of magnetic components in composition. But, the changes in imaginary and real parts of electrical permittivity in relation to frequency (within 1-18 GHz) for prepared composites at different annealing temperatures are illustrated in Fig. 6. Based on this figure, several point can be concluded as:

- The pure Ti_3C_2 MXene shows the highest values of real (ϵ') and imaginary part (ϵ'') of electrical permittivity.

- By increasing the annealing temperature to 700 °C, the real and imaginary part of electrical permittivity decrease progressively. This point can be related to the change in MXene structure and precipitation of TiO₂ phase within the Ti₃C₂ layers during annealing process.
- The changes in the imaginary and real parts of the electrical permittivity curves of the annealed samples at 700 and 800 °C are the same. This means that increasing the temperature further than 700 °C does not have a significant effect on the electrical permittivity of the resulting composites.
- The real and imaginary part of electrical permittivity of prepared composites follows a downward trend by increasing the frequency from 1 to 18 GHz. This is related to reductions in eddy currents losses [9].

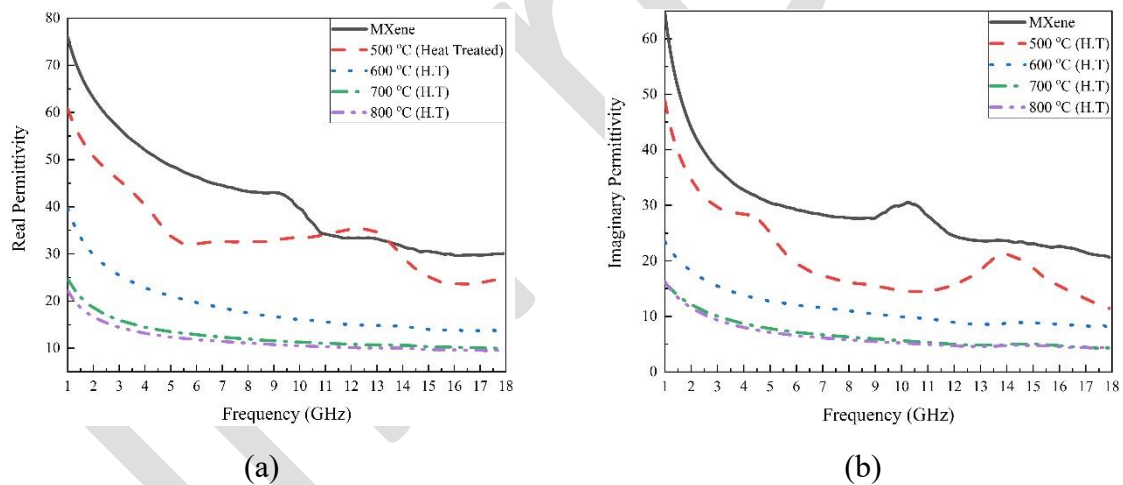


Fig. 6. The changes in a) imaginary and b) real parts of electrical permittivity in relation to frequency (within 1-18 GHz) for Ti₃C₂T_x MXene phase before and after annealing process at different annealing temperatures.

The attenuation coefficient (α) and skin depth (δ) are important parameters for evaluating the dissipating capacity and the microwave absorption capability of an electromagnetic wave absorber, respectively. The higher the attenuation coefficient of an absorber, the more

electromagnetic wave energy can be converted into heat. The skin depth values also affect the ability to absorb EM waves. The thickness of the absorbing material must be greater than the skin depth in order to positively affect the absorption performance of EM waves. The changes in attenuation coefficient and skin depth versus the frequency for prepared composites are shown in Fig. 7. The presented results in Fig. 7 are calculated using the following equations [9, 17]:

$$\alpha = \frac{\sqrt{2\pi f}}{c} \times \sqrt{(\mu''\epsilon'' - \mu'\epsilon') + \sqrt{(\mu''\epsilon'' - \mu'\epsilon')^2 - (\mu'\epsilon'' - \mu''\epsilon')^2}} \quad (6)$$

$$\sigma = 2\pi f \epsilon_0 \epsilon'' \quad (7)$$

$$\delta = \sqrt{\frac{1}{\pi f \mu \sigma}} \quad (8)$$

Where, C is the speed of light in vacuum, f denotes the incident wave frequency, σ is conductivity, ϵ_0 represents the electric permeability constant of the vacuum equal to 854.8×10^{-12} F/m.

Changes in damping constant relative to frequency for $\text{Ti}_3\text{C}_2/\text{TiO}_2$ composites are displayed in Fig.7 (a). Based on equation (6), higher ϵ'' result in a larger α value. Therefore, the highest and lowest values of α parameter correspond to pure $\text{Ti}_3\text{C}_2\text{T}_x$ MXene and annealed samples at 800°C , respectively. It should be noted that the value of parameter α decreases with increasing frequency. In other words, composites prepared at high frequency have higher performance.

According to the results presented in Fig. 7 (b), the values of δ decrease abruptly in the range of $1\text{--}7$ GHz, followed by an almost frequency-independent behavior. Based on this figure, it is quite evident that the maximum skin depth is related to $\text{Ti}_3\text{C}_2/\text{TiO}_2$ composites annealed at 800°C .

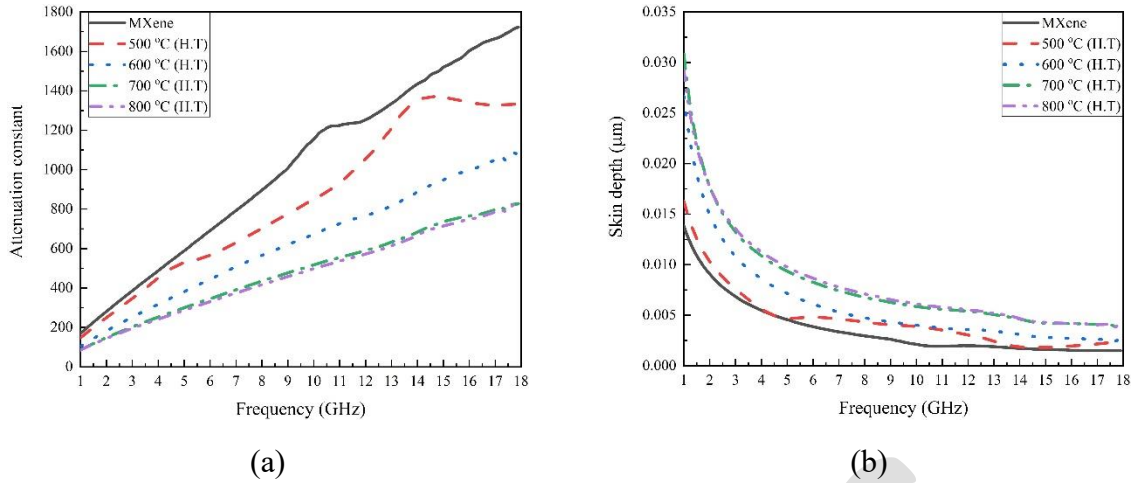


Fig. 7. The changes in a) attenuation constant and b) skin depth in relation to frequency (within 1-18 GHz) for $Ti_3C_2T_x$ MXene phase before and after annealing process at different annealing temperatures.

Reflection loss (RL) is a key parameter that characterizes the absorption characteristics of electromagnetic waves. When RL values are less than -10 dB, 90% of the EM wave energy is absorbed. EM wave absorption performance of prepared composites can be confirmed according to transmission line theory with RL value. It can be calculated by the correlation of complex permeability and complex permittivity as follows [9]:

$$RL(dB) = 20 \log \left| \frac{Z_{in} - Z_0}{Z_{in} + Z_0} \right| \quad (9)$$

$$Z_{in} = \sqrt{\frac{\mu_r}{\epsilon_r}} \tanh \left[j \frac{2\pi f t}{c} \sqrt{\mu_r \epsilon_r} \right] \quad (10)$$

Where Z_{in} is the input characteristic impedance, Z_0 denotes the impedance of free space, d stands for the thickness of the hybrid composite, ϵ_r shows the complex permittivity, μ_r represents the complex permeability.

In this regard, the RL curves of prepared composites at different temperatures within frequency range 1-18 GHz (1-5 mm thicknesses) are illustrated in Fig. 8. As seen, best absorption behavior of EM waves belongs to the annealed sample at 800 °C with a thickness of 2 mm with the RL_{min} of about -22 dB at matching frequency of 12 GHz. Meanwhile, the weakest absorption behavior

of EM waves, with RL_{min} of about -5.51 dB at matching frequency of 8.95 GHz, is attributed to the pure $Ti_3C_2T_x$ MXene phase. Considering that the RL_{min} of composites prepared at temperatures below 500 °C (-7.98 dB at matching frequency of 7.88 GHz) is less than -10 dB, these materials are not suitable for EM absorption. In contrast, performing annealing process at higher temperatures has been able to increase the performance of the resulting structures in absorbing electromagnetic waves to an acceptable extent. As seen, the reflection loss (RL) changed from -7.98 to -21.28 dB (within frequency range of $1-18$ GHz) with increasing in annealing temperature to about 800 °C. This result can be related to the increase in crystalline defects, reduction of interfaces and suitable percentage of TiO_2 within the Ti_3C_2 sheets.

According to Fig. 8, matching frequencies of prepared composites shift to lower frequencies with increasing sample thickness. The reason is attributed to the spin matching at high frequencies. In fact, the studied samples in this work follow the law of quarter-wavelength weakening as follow [17]:

$$t_m = \frac{n\lambda_m}{4} = \frac{nc}{4f_m\sqrt{|\mu_r||\epsilon_r|}} \quad (11)$$

In this equation, $n = 1, 2, 3$, f_m is the frequency corresponding to a particular RL peak, and λ_m denotes the wavelength at f_m [17]. Accordingly, the EM wave absorption function of the mentioned composites can be effectively adjusted by changing the thickness of the sample.

The data present in Table 1 have been presented for comparing the synthesized samples and some advanced ceramics. Evidently, electromagnetic parameters are heavily affected by the chemical composition and microstructure. For example, the Ti_3C_2/TiO_2 composites can be compared with Ti_3SiC_2/Al_2O_3 and $Ti_3C_2T_x/FCI$ [25, 26]. However, $Ti_3C_2T_x/Fe_3O_4$ because of existence of magnetic losses (μ' , μ'') shows a better electromagnetic behavior [27].

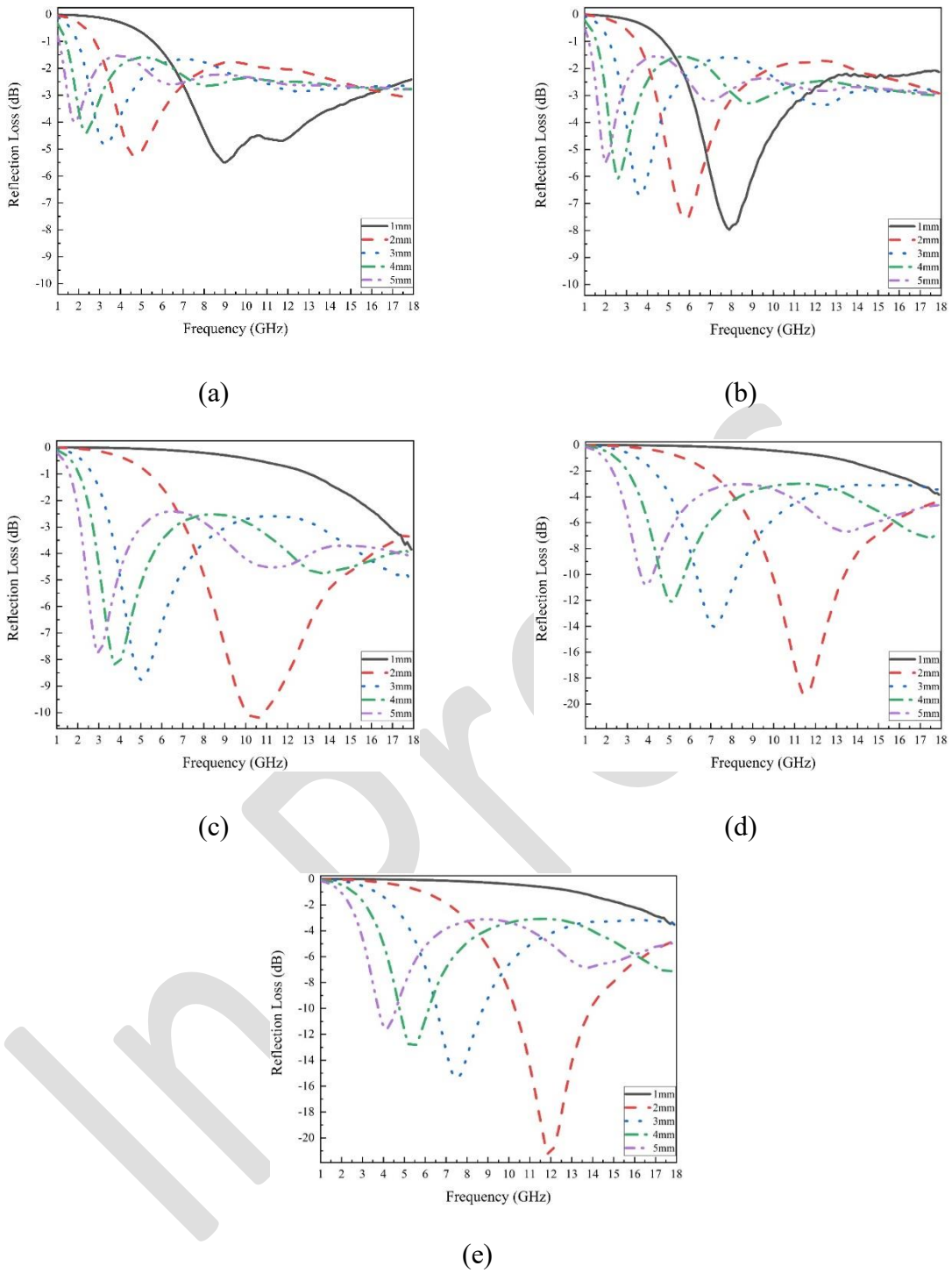


Fig. 8. Reflection loss (RL) curves related to $Ti_3C_2T_x$ MXene phase a) before and after annealing at b) 500, c) 600, d) 700 and e) 800 °C for 2 h .

Table 1. Comparison of EM wave absorbing properties of materials

| Sample | RL _{min} (dB) | Layer thickness (mm) | Ref. |
|---|------------------------|----------------------|------|
| Ti ₃ SiC ₂ /Al ₂ O ₃ | -16.4 | 2 | [25] |
| Ti ₃ C ₂ T _x /FCl | -15.52 | 1 | [26] |
| Ti ₃ C ₂ T _x /Fe ₃ O ₄ | -57.2 | 3.6 | [27] |

4. Conclusion

The present work, set out with the aim of studying the effect of TiO₂ on the electromagnetic (EM) behavior of in-situ Ti₃C₂/TiO₂ composites. The results showed that by performing the controlled annealing process, it is possible to deposit the TiO₂ particles within the MXene phase and form the Ti₃C₂/TiO₂ composites in situ. The electromagnetic wave absorbing behaviors of Ti₃C₂/TiO₂ composites is in direct relation with the annealing temperature as a result of the in-situ precipitation of TiO₂ within Ti₃C₂ sheets. The reflection loss (RL) changed from -7.98 to -21.28 dB (within frequency range of 1-18 GHz) with increasing in annealing temperature as well as increasing the size and percentage of formed TiO₂ phase.

Acknowledgments

I would like to thank Professor Ali Ghasemi for his invaluable feedback and reassurance, which influenced how I carried out my experiments, analyzed my results, and interpreted them.

Author contributions

All authors have participated in (a) conception and design, or analysis and interpretation of the data; (b) drafting the article or revising it critically for important intellectual content; and (c) approval of the final version.

Conflicts of interest

This manuscript has not been submitted to, nor is under review at, another journal or other publishing venue. The authors have no affiliation with any organization with a direct or indirect financial interest in the subject matter discussed in the manuscript. The authors have affiliations with organizations with direct or indirect financial interest in the subject matter discussed in the manuscript.

Data and code availability

“Not Applicable”

Supplementary information

“Not Applicable”

Ethical approval

“Not Applicable”

References

- [1] Wang, Z., Cheng, Z., Fang, C., Hou, X., Xie, L., “Recent advances in MXenes composites for electromagnetic interference shielding and microwave absorption”. *Composites Part A: Applied Science and Manufacturing*, 2020, 136, 105956-105973.
- [2] Lim, K.R.G., Shekhirev, M., Wyatt, B.C., Anasori, B., Gogotsi, Y., She, Z.W., “Fundamentals of MXene synthesis”. *Nature Synthesis*, 2022, 1(8), 601-614.
- [3] Heidarpour, A., Faraji, M., Haghghi, A., “Production and characterization of carbide-derived-nanocarbon structures obtained by HF electrochemical etching of Ti_3AlC_2 ”. *Ceramics International*, 2022, 48 (8), 11466-11474.

- [4] Shahin, N., Kazemi, Sh., Heidarpour, A., “*Mechanochemical synthesis mechanism of Ti_3AlC_2 MAX phase from elemental powders of Ti, Al and C*”. *Advanced Powder Technology*, 2016, 27 (4), 1775-1780.
- [5] Aghamohammadi, H., Heidarpour, A., Jamshidi, R., Ghasemi, S., “*Study on the chemical stability of the synthesized TiC_x in Ti-Al-C system after immersion in the $HF+H_2O_2$ solution*”. *Advanced Powder Technology*, 2019, 30 (2), 393-398.
- [6] Pan, F., Yu, L., Xiang, Z., Liu, Z., Deng, B., Cui, E., Shi, Z., Li, X., Lu, W., “*Improved synergistic effect for achieving ultrathin microwave absorber of 1D Co nanochains/2D carbide MXene nanocomposite*”. *Carbon*, 2021, 172, 506-515.
- [7] Wang, X., Zhao, C., Li, C., Liu, Y., Sun, S., Yu, Q., Yu, B., Cai, M., Zhou, F., “*Progress in MXene-based materials for microwave absorption*”. *Journal of Materials Science & Technology*, 2024, 180, 207-225.
- [8] Guan, X., Yang, Z., Zhou, M., Yang, L., Peymanfar, R., Aslibeiki, B., Ji, G., “*2D MXene nanomaterials: Synthesis, mechanism, and multifunctional applications in microwave absorption*”. *Small Structures*, 2022, 3(10), 2200102-2200125.
- [9] Ghasemi, A., *Magnetic Ferrites and Related Nanocomposites*, Elsevier, USA, 2022.
- [10] Chang, M., Li, Q., Jia, Z., Zhao, W., Wu, G., “*Tuning microwave absorption properties of $Ti_3C_2T_x$ MXene-based materials: Component optimization and structure modulation*”. *Journal of Materials Science & Technology*, 2023, 148, 150-170.
- [11] Kumar, A., Agarwala, V., Singh, D., “*Microwave absorbing behavior of metal dispersed TiO_2 nanocomposites*”. *Advanced Powder Technology*, 2014, 25 (2), 483-489.
- [12] Liu, Z., Zhou, Y., Yang, L., Yang, R., “*Green preparation of in-situ oxidized TiO_2/Ti_3C_2 heterostructure for photocatalytic hydrogen production*”. *Advanced Powder Technology*, 2021, 32 (12), 4857-4861.

- [13] F. Wang, C. Yang, M. Duan, Y. Tang, J. Zhu, TiO₂ nanoparticle modified organ like Ti₃C₂ MXene nanocomposite encapsulating hemoglobin for a mediator-free biosensor with excellent performances, *Biosensors and Bioelectronics* 74 (2015) 1022-1028.
- [14] Tong, Y., He, M., Zhou, Y., Nie, S., Zhong, Q., Fan, L., Huang, T., Liao, Q., Wang, Y., “Three-dimensional hierarchical architecture of the TiO₂/Ti₃C₂T_x/RGO ternary composite aerogel for enhanced electromagnetic wave absorption”. *ACS sustainable chemistry & engineering*, 2018, 6 (7), 8212-8222.
- [15] Fan, B., Shang, S., Dai, B., Zhao, B., Li, N., Li, M., Zhang, L., Zhang, R., Marken, F., “2D-layered Ti₃C₂/TiO₂ hybrids derived from Ti₃C₂ MXenes for enhanced electromagnetic wave absorption”. *Ceramics International*, 2020, 46 (10), 17085-17092.
- [16] Sun, X., Zhao, X., Zhang, X., Wu, G., Rong, X., Wang, X., “TiO₂ nanosheets/Ti₃C₂T_x MXene 2D/2D composites for excellent microwave absorption”, *ACS Applied Nano Materials*, 2023, 6 (15), 14421-14430.
- [17] Yan, H., Guo, Y., Bai, X., Qi, J., Lu, H., “Facile constructing Ti₃C₂T_x/TiO₂@C heterostructures for excellent microwave absorption properties”. *Journal of Colloid and Interface Science*, 2024, 654, 1483-1491.
- [18] Gao, Y., Du, H., Li, R., Zhang, Q., Fan, B., Zhao, B., Li, N., Wang, X., Chen, Y., Zhang, R., “Multi-phase heterostructures of flower like Ni (NiO) decorated on two-dimensional Ti₃C₂T_x/TiO₂ for high-performance microwave absorption properties”. *Ceramics International*, 2021, 47 (8), 10764-10772.
- [19] Zamani, K., Tavoosi, M., Ghasemi, A., Gordani, G., “Electromagnetic characterization of MAX phase and MXene in Ti-Al-C ternary system”, *Materials Chemistry and Physics*, 2024, 323, 129622-129632.

- [20] Tahir, M., “*Nanoconfined $Ti_3C_2@$ in situ grown TiO_2 and ruthenium triphenylphosphine (Ru-II) coupled g- C_3N_4 to construct $RuP-Ti_3C_2@TiO_2/EC_3N_4$ dual function nanocomposite for enhancing photocatalytic green hydrogen production*”. *Chemical Engineering Journal*, 2023, 476, 146680-146690.
- [21] Tong, Y., He, M., Zhou, Y., Zhong, X., Fan, L., Huang, T., Liao, Q., Wang, Y., “*Electromagnetic wave absorption properties in the centimetre-band of $Ti_3C_2T_x$ MXenes with diverse etching time*”, *Journal of Materials Science: Materials in Electronics*, 2018, 29, 8078-8088.
- [22] Lei, B., Huang, X., Wu, P., Wang, L., Huang, J., Wang, Z., “*Sandwich-like preparation of $Ti_3C_2T_x/CoFe/TiO_2$ nanocomposites for high-performance electromagnetic wave absorption*”. *Ceramics International*, 2022, 48 (17), 25111-25119.
- [23] Yang, J.X., Yu, W.B., Li, C.F., Dong, W.D., Jiang, L.Q., Zhou, N., Zhuang, Z.P., Liu, J., Hu, J.Y., Zhao, H., “*PtO nanodots promoting Ti_3C_2 MXene in-situ converted Ti_3C_2/TiO_2 composites for photocatalytic hydrogen production*”. *Chemical Engineering Journal*, 2021, 420, 129695-129704.
- [24] Zhou, C., Wang, X., Luo, H., Deng, L., Wei, S., Zheng, Y., Jia, Q., Liu, J., “*Rapid and direct growth of bipyramid TiO_2 from $Ti_3C_2T_x$ MXene to prepare $Ni/TiO_2/C$ heterogeneous composites for high-performance microwave absorption*”. *Chemical Engineering Journal*, 2020, 383, 123095-123104.
- [25] Dai, B., Zhao, B., Xie, X., Su, T., Fan, B., Zhang, R., Yang, R., “*Novel two-dimensional $Ti_3C_2T_x$ MXenes/nano-carbon sphere hybrids for high-performance microwave absorption*”. *Journal of Materials Chemistry C*, 2018, 6, 5690-5697.
- [25] Zhang, X., Wang, H., Hu, R., Huang, C., Zhong, W., Pan, L., Feng, Y., Qiu, T., Zhang, C.J., Yang, J., “*Novel solvothermal preparation and enhanced microwave absorption*

properties of $Ti_3C_2T_x$ MXene modified by in situ coated Fe_3O_4 nanoparticles". *Applied Surface Science*, 2019, 484, 383-391.

[26] Yan, S., Cao, C., He, J., He, L., Qu, Z., "Investigation on the electromagnetic and broadband microwave absorption properties of Ti_3C_2 Mxene/flaky carbonyl iron composites". *Journal of Materials Science: Materials in Electronics*, 2019, 30, 6537-6543.

[27] Zhao, D., Xia, S., Wang, Y., Wang, M., "High-performance microwave absorption properties of Ti_3SiC_2/Al_2O_3 coatings prepared by plasma spraying". *Applied Physics A*, 2020, 126, 1-9.

In Press